02

Josephson effect in FeSe point contacts

© *M.V. Golubkov*[1], *V.A. Stepanov*[1], *A.V. Sadakov*[1], *A.S. Usoltsev*[1], *D.A. Chareev*[2,3,4]

[1] Lebedev Physical Institute, Russian Academy of Sciences,
Moscow, Russia
[2] Korzhinsky Institute of Experimental Minerology, Russian Academy of Sciences,
Chernogolovka, Moscow Region, Russia
[3] Dubna State University,
Dubna, Moscow region, Russia
[4] Institute of Physics and Technology, Ural Federal University,
Ekaterinburg, Russia

E-mail: golubkov@lebedev.ru

Received May 16, 2025
Revised May 27, 2025
Accepted May 27, 2025

The paper presents the results of studies of PbIn/FeSe and FeSe/FeSe Josephson point contacts tuned in helium with critical currents $I_C(4.2\,K) = 1.80-0.43$ mA and characteristic voltages $V_C(4.2\,K) = 0.057-0.144$ mV. The dependences of V_C of contacts on temperature T and the dependences of the amplitudes of the current steps on the current-voltage characteristics on the power of electromagnetic radiation P_{MW} with a frequency of 8 GHz were measured. The $V_C(T)$ dependences were well approximated by the known models of SS′S, SIS contacts. The dependences of the amplitudes of the first steps of the contact current on P_{MW} were described by a resistive model with a current proportional to $\sin(\varphi)$ with a normalized frequency of microwave radiation found from the oscillation period of the current steps. The obtained results unambiguously indicated the usual s — symmetry of the order parameters in the FeSe bands

Keywords: iron-based superconductors, order parameter, Josephson effect, resistive model.

DOI: 10.61011/PSS.2025.05.61484.124-25

1. Introduction

FeSe — is the simplest in structure and probably the most unusual superconductor by its properties in the family of iron-based superconductors [1–5]. The current research methods found many characteristics of this multiband metal. Study of Shubnikov–de Haas [6] oscillations, ARPES [7], temperature dependences of heat capacity [8], penetration depth of magnetic field [9], data of tunnel spectroscopy and Andreev reflection [10–14], temperature dependences of critical magnetic field $H_{C2}(T)$ [15,16] revealed the main characteristics of superconducting and normal FeSe states. Theoretical calculations correlate well with the measurements. At the same time the coupling interaction and order parameter (OP) symmetry closely related to it, despite many experimental and theoretical studies, have not yet been established. The possible OP symmetries considered were standard s, d, mixed symmetries $s + d$, $s + id$. Currently the most probable OP symmetry of FeSe is $s^{\pm}$ — symmetry related to coupling spin fluctuations [17–20]. This symmetry suggests different OP signs (phase difference is equal to π) in the bands that participate in formation of a superconducting condensate. Experimental estimates of FeSe OP symmetry did not allow this characteristic to be unambiguously determined.

OP symmetry is closely related to interband interaction of superconducting condensates reflecting as well on the dependences of energy gaps and critical magnetic fields of bands on temperature [9,11–15]. Study of the penetration depth of the magnetic field [9] and tunnel measurements [11–13], have shown practically complete absence or very weak interband interaction in FeSe, therefore, a conclusion on ordinary s-OP symmetries in the bands follows. At the same time, measurements of temperature dependences of energy gaps $\Delta_{1,2}(T)$ in paper [14] and temperature dependences $H_{C2}(T)$ [15] in the magnetic field of various orientation with induction to 38 T at temperatures of down to $T/T_C \approx 0.4$ demonstrated that the obtained results are approximated by theoretical dependences within a two-band isotropic model within a pure limit only with account of noticeable interband scattering. From these measurements it follows that $s\pm$-OP symmetry is also possible. New information on FeSe OP symmetry may be provided by measurements sensitive to OP phase. The only measurable value sensitive to the superconductor OP phase is the current in the Josephson contact [21], which at standard s-OP symmetry is directly proportional to the sinus of OP phase difference of the contact electrodes φ [22]. Theoretical estimates have shown that at $s\pm$ — OP symmetry the following is possible: 1) appearance of members in the current via the contact that are proportionate to $\sin(2\varphi)$; 2) deviations from the dependences of Josephson contact characteristic voltage on temperature known for s-symmetry[23–28].

The first consequence of $s\pm$-symmetry must result in appearance of the brightest feature of Josephson contact current — subharmonic steps in CVC in the high-frequency electromagnetic radiation field [23–28]. Experimental studies of the Josephson effect in point and planar contacts with Fe-pnictides of different families have shown, in the vast majority of experiments, the standart s-OP symmetry in these compounds [29–39]. Nevertheless, until now there have been no measurements of Josephson effect characteristics in contacts with FeSe.

This paper presents the results of Josephson current studies in the point contacts (PC) adjusted in liquid helium conventional superconductor PbIn/FeSe (NA — needle-anvil PC) and FeSe/FeSe contacts in a break junction PC (BJ) in FeSe crystals. Current-voltage curves (CVC) of PC were measured with different resistances and critical currents I_C, dependences of characteristic voltage of PC $V_C = I_C \times R_N$ on temperature (R_N — PC resistance in normal state), dependences of the first current steps in CVC (I_n, $n = 0, 1, 2$; $I_{n=0} = I_C$) on the power of microwave radiation. The measured dependences were approximated by suitable theoretical models. The objective of the paper was to evaluate the FeSe OP symmetry.

2. Experiment procedure

To create PC, we used the same FeSe crystals [40], as in our paper [14]. Single-crystal FeSe plates with dimensions of up to $1.2 \times 0.7\,\mathrm{mm}^2$ and thicknesses of $0.08-0.03\,\mathrm{mm}$, were obtained by exfoliating of one relatively thick crystal. Critical temperature, width of superconducting transition, residual resistance, ratio of residual resistivity at 300 and 11 K were equal accordingly to $T_C = 9.2\,\mathrm{K}$, $\Delta T_C = 0.3\,\mathrm{K}$ (by magnetic susceptibility), $\rho(11\,\mathrm{K}) \approx 28\,\mu\Omega \cdot \mathrm{cm}$, $R(300\,\mathrm{K})/R(11\,\mathrm{K}) = 23$. These values were close to characteristics of best crystals [1,41–43] and proved high quality of the specimens.

As a conventional superconductor we used, as before, $\mathrm{Pb}_{1-x}\mathrm{In}_x$ with $T_C^{\mathrm{PbIn}} = 6.2-6.4\,\mathrm{K}$ and $\Delta T_C = 0.1\,\mathrm{K}$. Methods to create PC of needle-anvil type [44] (NA) and contacts on a break junction (BJ), cryogenic and electronic equipment are described in detail in our publications [14,38,39]. All measurements were carried out in an homemade insert to a transport He Dewar, making it possible to do measurements in the temperature range of $1.8-10\,\mathrm{K}$, to stabilize the temperature with the precision of 0.01 K, to study the characteristics of the contact in the field of microwave radiation with frequency of $6-12\,\mathrm{GHz}$. Theoretical models were adjusted to the measured dependences using curvefit software.

3. Results and discussion

NA and BJ PCs were created after crystal cooling down to $1.8-2\,\mathrm{K}$. As a rule, at the first touch of the NA PC electrodes, the critical current was absent, and the resistance was from several dozens to hundreds of Ohms. As pressure of the „needle" ($\mathrm{Pb}_{1-x}\mathrm{In}_x$) on the crystal increases, the PC resistance dropped, and critical current appeared on the current-voltage curve (CVC) I_C. PC was adjusted for $I_C \approx 0.4-1.8\,\mathrm{mA}$. To create a BJ PC, a FeSe crystal fixed on a springy base, was first broken, and then the PC current was adjusted to the required value by variation of the pressure at the base. To test the Josephson nature, the PC contact was radiated with high-frequency electromagnetic radiation. At the same time, current steps appeared on CVC — this proved that the connection between the PC electrodes was weak. After checking the stability and properties of the PC in a microwave field of different power, the CVC were recorded at a minimum temperature and with an increase in microwave power, and then with an increase in temperature from the minimum to the critical in the absence of microwave radiation.

Typical CVCs for our PCs at different temperatures T are shown in Figure 1, *a*, at different powers of microwave radiation P_{MW} — in Figure 1, *b*. Stability of contacts proved the coinside of CVCs recorded prior to the start of the change T or P_{MW}, and after the end of the series recording and return to the initial corresponding values. PC stability testing was mandatory for any series of measurements. CVC (Figure 1, *b*) shows well the change of amplitudes of the first current steps depending on P_{MW}.

Recorded CVCs: 1) differed from hyperbolic ones, typical for the resistive model of Josephson's contact; 2) were asymmetrical as a rule $+I_C \neq -I_C$; 3) had a smoothened transition from $V = 0$ to $V \neq 0$, which practically did not depend on the value of the critical current, temperature and power of a microwave signal; 4) had low normal resistance $R_N \approx 0.05-0.1\,\Omega$; 5) had a small, around 0.1 mV, value of characteristic voltage $V_C = I_C \times R_N$.

Such features of CVCs were noted previously both for point and planar contacts of relatively large area, where a weak bond between PC electrodes was provided by a series of micro-bridges of SNS type, SS′S, SIS′IS... (here S′ — thin superconducting, N — „normal" metal interlayer between massive S PC electrodes with the critical temperature $T_C^{'} < T_C$, length $L \gg \xi^*$ (ξ^* — coherence length in S′ (N) bridge), I — insulator) [45–48]. It should be noted that there were no features in CVCs associated with the correlated motion of vortices, the second harmonic in the $I(\varphi)$ dependence, and the presence of stimulation of superconductivity [49].

Typical dependences of the characteristic voltage $V_C = I_C \times R_N$ on temperature are shown with symbols for BJ PC in Figure 2, *a*, for NA PC in Figure 2, *b*. Value I_C was assessed by the crossing point of the straight line approximating CVC in the range of $20-60\,\mu\mathrm{V}$ with y-axis, R_N — by the slope of this line. The sharp difference in the $V_C(T)$ dependencies for NA and BJ PC is striking.

Dependences $V_C(T)$ BJ PC (Figure 2, *a*) are very similar to the corresponding dependences of long „dirty" SS′S, SIS′IS or SNS bridges — narrow conducting N or S′ channels between S electrodes of the contact. In the limit of „dirty" electrodes and bridge material (mean free path l is much smaller than the coherence length in electrodes ξ and

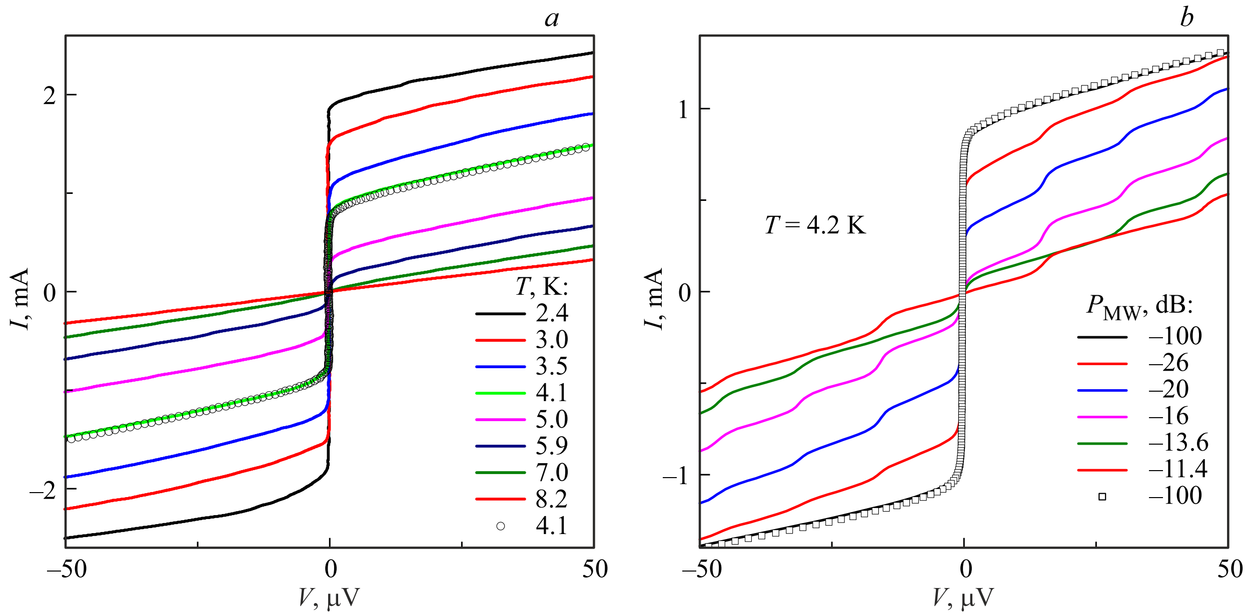

Figure 1. Typical CVCs for PCs at different temperatures T (a) and powers of microwave radiation P_{MW} (b).

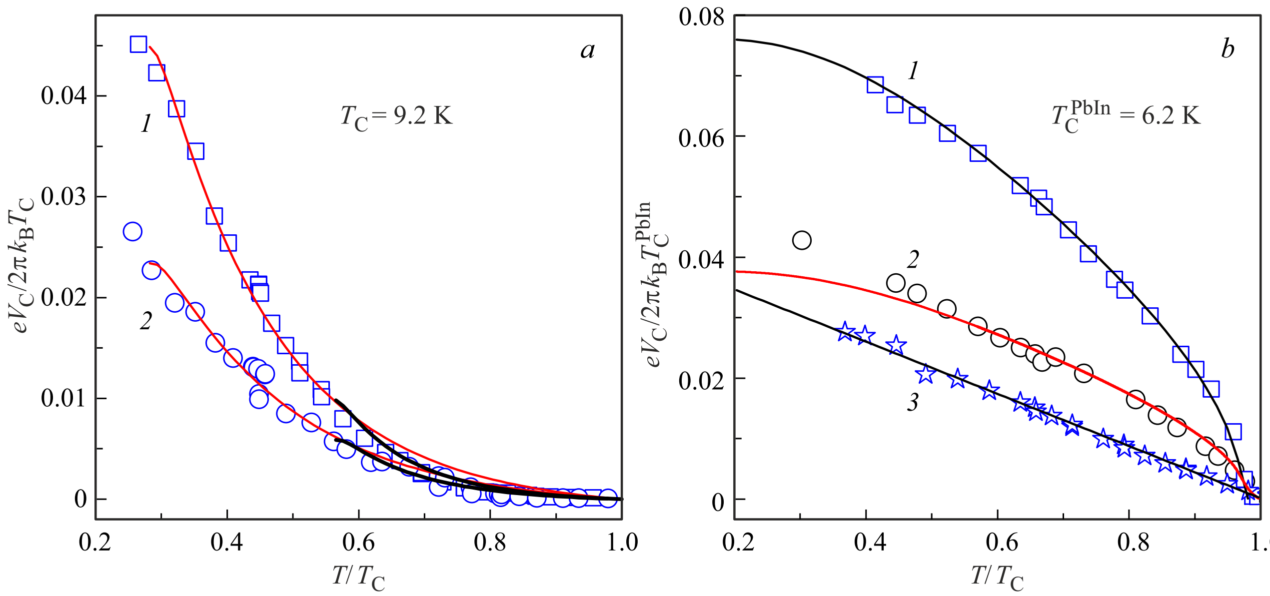

Figure 2. Dependences of normalized characteristic voltage on temperature: a) for BJ PC (symbols), lines — result of adjustment in the model of SS′S contact (Table 1); b) for NA PC (symbols), lines — result of adjustment in the model of SIS contact (Table 2) for dependences *1* and *2*, for dependence *3* it shows the result of adjustment with a straight line.

bridge ξ^*) de Genne [50] showed that under strict boundary conditions (there is no suppression of superconductivity in electrodes) the characteristic voltage for the bridge with length $L \gg \xi^*$ in the wide range of temperatures $T < T_{\mathrm{C}}$:

$$V_{\mathrm{C}}(T) = I_{\mathrm{C}} \times R_{\mathrm{N}} \propto \exp\left[-\frac{L}{\xi^*(T)}\right], \quad L \gg \xi^*. \tag{1}$$

The calculation of V_{C} of long bridges ($L \gg \xi^*$) from Usadel's microscopic theory for „dirty“ superconductors in [21,51–54] refined the de Genne formula. Dependence $V_{\mathrm{C}}(T)$ for $T > T'_{\mathrm{C}}$ (T'_{C} — critical temperature of bridge material) may be calculated from the following ratios:

$$V_{\mathrm{C}} = \frac{2\pi k_{\mathrm{B}} T_{\mathrm{C}}}{e} V^* \frac{L}{\xi^*} \exp\left[-\frac{L}{\xi^*}\right]; \quad L \gg \xi^*, \tag{2}$$

$$V^* = \frac{32 k_{\mathrm{B}} T}{e T'_{\mathrm{C}}} \frac{\Delta^2}{\left[\pi k_{\mathrm{B}} T + \Delta^* + \sqrt{2\Delta^*(\pi k_{\mathrm{B}} T + \Delta^*)}\right]^2},$$

$$\Delta^* = \sqrt{(\pi k_{\mathrm{B}} T)^2 + \Delta^2}, \quad \xi^* = \xi \sqrt{\frac{T_{\mathrm{C}}}{T}\left[1 + \frac{\pi^2}{4} \ln^{-1} \frac{T}{T_{\mathrm{C}}}\right]}.$$

In formulae (2) T_C, Δ and ξ — critical temperature, energy gap and coherence length in PC electrodes, e — electron charge, k_B — Boltzmann constant. Despite the multi-band nature of FeSe and the lack of consideration of interband scattering in this model, we try to use formulae (2) to approximate the dependences we measured. Energy gaps and critical temperature of FeSe, in accordance with our measurements, are equal to: $\Delta_1 = 2.06$ meV, $\Delta_2 = 0.68$ meV, $T_C = 9.2$ K [14]. Let us take the following as variable parameters: critical temperature T'_C, ratio of bridge length to coherence length of FeSe L/ξ and coefficient g — ratio of theoretical characteristic voltage to experimental one. Introduction of coefficient g is related to the fact that characteristic voltage of Josephson's contacts with electrodes from Fe-based superconductors is substantially lower than value k_BT_C, specific for conventional superconductors [28–38]. The reasons for such phenomenon have not yet been finalized. Variable values obtained from approximation of dependences $V_C(T)$ for two different PCs are provided in Table 1.

The dependences $V_C(T)$ produced from approximation are shown in Figure 2, *a* with the lines. You can see that in the adjustment to the narrow temperature range $T_C > T > T'_C \approx 5$ K the calculated dependence reproduced the experimental one well. As the temperature range expanded to 2.4 K, the approximation accuracy remained acceptable. Substitution in formulae (2) of Δ_1 for Δ_2 resulted only in the change of the ratio L/ξ, not affecting the approximation accuracy.

Dependences $V_C(T)$ NA PC differed by high diversity (Figure 2, *b*): the shape of the measured dependences varied from a convex to a straight line. The straight line of dependence $V_C(T)$ near the critical temperature $(T_C - T) \ll T_C$ is specified for classic SIS structures and micro-bridges with $L \approx 0$ [21,22,54,55], where $V_C(T)$ is proportional to the product of energy gaps of PC electrodes $\Delta_1(T)\Delta_2(T) \propto (T_C - T)$ [54,55]. For one of our PCs $V_C(T) \propto (T_C - T)$ in the entire measurement range (dependence *3* of Figure 2, *b*) is up to $T = 0.37\,T_C$. Such dependences $V_C(T)$ were noted previously for planar contacts, too [29,56]. There is no theoretical model causing linear dependence $V_C(T)$ in the wide temperature range.

Dependences *1* and *2* in Figure 2, *b* are closer to dependence of Ambegaokar–Baratoff [55] for tunnel contacts. We will try to use this model with account of a two-zone nature of FeSe. Current from PbIn ($\Delta_{\mathrm{PbIn}} = 0.98$ meV) goes to zone *1* ($\Delta_1 = 2.06$ meV) and zone *2* ($\Delta_2 = 0.62$ meV) FeSe. Full current of PC I_C is equal to the sum of currents in *1* and *2* FeSe zone. Such model of Josephson's contact is considered in paper [57]:

$$I_C = I_{C1} + I_{C2};\; R_N = \frac{R_{N1}R_{N2}}{R_{N1} + R_{N2}},$$

$$V_C(T) = I_C R_N(T) = I_{C1}R_{N1}(T)\,\frac{1}{1+\alpha} + I_{C2}R_{N2}(T)\,\frac{\alpha}{1+\alpha};$$

$$\alpha = \frac{R_{N1}}{R_{N2}}, \tag{3}$$

Table 1. Parameters of SS′S contact model

№ of dependence in Figure 2, *a*	T'_C, K	L/ξ	g
1	2.42	10.7	0.126
	5.03	12.5	0.026
2	2.37	10.3	0.068
	5.07	12.0	0.015

Table 2. Variable parameters of SIS contact model

№ of dependence in Figure 2, *b*	α	T_C^{PbIn}, K	g
1	26.80	6.15	0.209
2	79.39	6.13	0.107

$$I_{C1,2}R_{N1,2}(T) = \frac{\pi k_B T}{e}\,\Delta_{\mathrm{PbIn}}\Delta_{1,2} \times \sum_{m=-\infty}^{m=\infty}\left[(\omega_m^2 + \Delta_{\mathrm{PbIn}}^2)(\omega_m^2 + \Delta_{1,2}^2)\right]^{-0.5},$$

$$\omega_m = 2\pi k_B T(2m+1),$$

where R_{N1} and R_{N2} — resistances of current channels to zones *1* and *2* FeSe, $\Delta_{1,2}(T)$ — FeSe energy gaps, m — integer number.

The variable parameters used were α, T_C^{PbIn} and g, at the same time it was deemed that $\Delta_{\mathrm{PbIn}}(T)$ follows BCS dependence, temperature dependences of FeSe energy gaps $\Delta_{1,2}(T)$ were measured by us previous and differ from BCS [14]. The result of approximation of dependences *1* and *2* is shown in Figure 2, *b* with the lines.

Table 2 provides values of adjustable parameters produced from approximation for two NA PC. Since $\alpha \gg 1$, then FeSe zone with the energy gap $\Delta_1 = 2.06$ meV practically does not impact the characteristics of contacts.

Figure 3 uses symbols to show dependences of normalized critical current ($n = 0$) and first steps of current ($n = 1, 2$) on power of microwave radiation $i_n^{\exp}(\sqrt{P_{\mathrm{MW}}})$ in NA and BJ PC. You can see that at certain powers P_{MW} the current steps i_n were fully suppressed. This proves the absence of currents of non-Josephson nature in PC. The measured dependences were approximated with the ones calculated from the equation of the resistive model of Josephson's contact with the superconducting current $I_S = I_C \sin(\varphi)$. Calculation of CVC contact reduced to solving a differential equation [22,58]:

$$\frac{d\varphi}{d\tau} = i + i_{\mathrm{ac}}\sin\Omega\tau - \sin\varphi, \tag{4}$$

$$\tau = \left(\frac{2e}{\hbar}\,I_C R_N\right)t;\quad \Omega = 2\pi f \Big/ \left(\frac{2e}{\hbar}\,I_C R_N\right),$$

where i and i_{ac} — direct and alternating currents, normalized by I_C, τ — normalized time, Ω — normalized

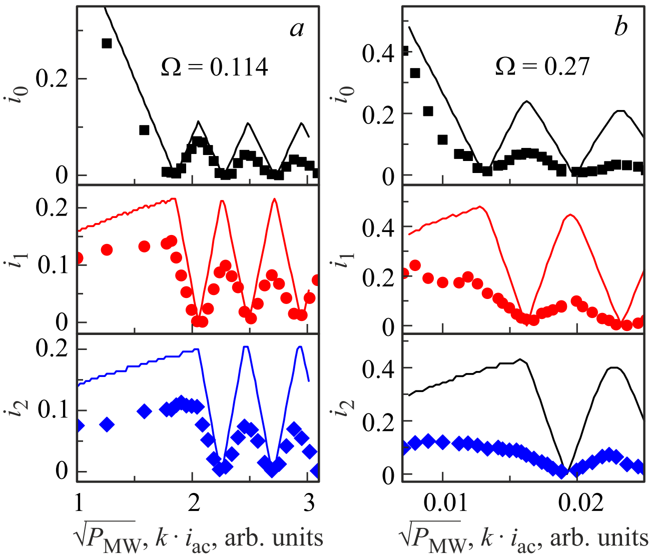

Figure 3. Symbols — measured dependences of critical current ($n = 0$) and the first steps of current ($n = 1, 2$) on power of microwave radiation $i_n^{\exp}(\sqrt{P_{MW}})$ in NA (a) and BJ (b) PC. Dependences calculated according to the formulae of the resistive model $i_n^{\text{calk}}(i_{ac})$ are shown in these figures with the lines. Coefficient k matches the measured and calculated dependences.

frequency of electromagnet radiation f. The solution to this equation is the dependence $\varphi(\tau)$ and normalized to V_C direct voltage v, equal to the time-averaged oscillations of Josephson's alternating current $v = \langle d\varphi/d\tau \rangle(i)$, i.e. normalized CVC. At $i_{ac} > 0$ in CVC at $v = n\Omega$ current steps occurred, the amplitude of which $i_n^{\text{calk}}(i_{ac})$ $(n = 0, 1, 2, \ldots)$ was determined by value i_{ac}.

In equation (4) the only value to be found from the measured characteristics of PC, is the normalized frequency Ω, related to the characteristic voltage of contact V_C. Study of the Josephson's contacts with the electrodes from iron-based superconductors [38,39] showed that the standard method for definition of V_C according to CVC does not work. The accurate value Ω may easily be determined from the normalized periods of oscillations $\eta_n = (i_n^{(2)} - i_n^{(1)})/i_n^{(1)}$ $(n = 0, 1, 2)$ of the first steps of current in the field of microwave radiation [59,60]. $i_n^{(1)}$ and $i_n^{(2)}$ in this formula are the first and second minima on the dependence of n-th current step $i_n^{\exp}(\sqrt{P_{MW}})$. The relationship η_n with Ω for the first current steps of CVC, following from the RSJ model with $I_S = I_C \sin(\varphi)$, was calculated in paper [59]. In paper [60] the calculated dependences were approximated by polynomials making it possible to easily find $\Omega(\eta_n)$ for steps with $n = 0, 1, 2$ with accuracy of $\approx 1\,\%$. This method works for Josephson's contacts of any type, regardless of the shape and features of CVC. For the dependences shown by symbols in Figure 3, $\Omega = 0.114$ and 0.27.

The calculated dependences $i_n^{\text{calk}}(k i_{ac})$ were shown in Figure 3 with the lines. Coefficient k was selected so that for the first current step the first minima of oscillations $i_1^{(1)}$ coincided. You can see that the periods of measured and calculated dependences coincide well. This proves the applicability of the resistive model of PC with $I_S = I_C \sin(\varphi)$ for CVC description in the field of microwave radiation. The proportionality of superconducting current of contacts $\sin(\varphi)$ confirms the regular, s-symmetry of OP in FeSe.

4. Conclusion

Stable Josephson's point contacts PbIn/FeSe (NA) and FeSe/FeSe (BJ) were created. Current-voltage curves of all obtained PCs were noticeably different from those calculated from the resistive model. Dependences of the characteristic voltage of contacts $V_C(T) = I_C R_N$ on temperature and dependences of amplitudes of current steps in CVC in the field of microwave radiation on radiation power $I_n(P_{MW})$ $(n = 0, 1, 2)$ were measured. It was shown that NA PCs had the structure close to the tunnel superconductor–insulator–superconductor (SIS), and BJ PCs — the structure of the bridge SS′S with length of $L \gg \xi^*$ (coherence lengths in S′ layer). Oscillations of current steps in CVC were described well with the resistive model of PC with Josephson's current, proportional to $\sin(\varphi)$. Approximations of all measured dependences (qualitatively) are possible using well-known models. The obtained results indicate ordinary s (s^{++})-symmetry of order parameter FeSe.

Funding

The study was partially supported by the project of the Russian Science Foundation 22-72-10034. A.B.C. gratefully acknowledges the financial support from the project of the Russian Science Foundation 23-12-00307. Growth of crystals is financed by the Ministry of Science and Higher Education of the Russian Federation and Development Program of the Ural Federal University within Priority-2030 and FMUF-2022-0002.

Acknowledgments

The authors are sincerely grateful to the employees of the Solid State Science Department, Physical Institute of Academy of Sciences for the assistance in performance of this study.

Conflict of interest

The authors declare that they have no conflict of interest.

References

[1] S. Kasahara, T. Watashige, T. Hanaguri, Y. Kohsaka, T. Yamashita, Y. Shimoyama, Y. Mizukami, R. Endo, H. Ikeda, K. Aoyama, T. Terashima, S. Uji, T. Wolf, H. von Löhneysen, T. Shibauchi, Y. Matsuda. PNAS **111**, *46*, 16309 (2014).

[2] X. Liu, L. Zhao, S. He, J. He, D. Liu, D. Mou, B. Shen, Y. Hu, J. Huang, X.J. Zhou. J. Phys. Condens. Matter **27**, *18*, 183201 (2015).

[3] A. Krzton-Maziopa, V. Svitlyk, E. Pomjakushina, R. Puzniak, K. Conder. J. Phys. Condens. Matter **28**, *29*, 293002 (2016).
[4] T. Shibauchi, T. Hanaguri, Y. Matsuda. J. Phys. Soc. Jpn. **89**, *10*, 102002 (2020).
[5] R. Liu, M.B. Stone, S. Gao, M. Nakamura, K. Kamazawa, A. Krajewska, H.C. Walker, P. Cheng, R. Yu, Q. Si, P. Dai, X. Lu. arXiv: 2401.05092.
[6] T. Terashima, N. Kikugawa, A. Kiswandhi, E.-S. Choi, J.S. Brooks, S. Kasahara, T. Watashige, H. Ikeda, T. Shibauchi, Y. Matsuda, T. Wolf, A.E. Böhmer, F. Hardy, C. Meingast, H. Löhneysen, M.-T. Suzuki, R. Arita, S. Uji. Phys. Rev. B **90**, *14*, 144517 (2014).
[7] D. Liu, C. Li, J. Huang, B. Lei, L. Wang, X. Wu, B. Shen, Q. Gao, Y. Zhang, X. Liu, Y. Hu, Y. Xu, A. Liang, J. Liu, P. Ai, L. Zhao, S. He, L. Yu, G. Liu, Y. Mao, X. Dong, X. Jia, F. Zhang, S. Zhang, F. Yang, Z. Wang, Q. Peng, Y. Shi, J. Hu, T. Xiang, X. Chen, Z. Xu, C. Chen, X.J. Zhou. Phys. Rev. X **8**, *3*, 031033 (2018).
[8] Y. Sun, S. Kittaka, S. Nakamura, T. Sakakibara, K. Irie, T. Nomoto, K. Machida, J. Chen, T. Tamegai. Phys. Rev. B **96**, *22*, 220505(R) (2017).
[9] R. Khasanov, M. Bendele, A. Amato, K. Conder, H. Keller, H.-H. Klauss, H. Luetkens, E. Pomjakushina. Phys. Rev. Lett. **104**, *8*, 087004 (2010).
[10] C.-L. Song, Y.-L. Wang, P. Cheng, Y.-P. Jiang, W. Li, T. Zhang, Z. Li, K. He, L. Wang, J.-F. Jia, H.-H. Hung, C. Wu, X. Ma, X. Chen, Q.-K. Xue. Science **332**, *6036*, 1410 (2011).
[11] Y.G. Ponomarev, S.A. Kuzmichev, T.E. Kuzmicheva, M.G. Mikheev, M.V. Sudakova, S.N. Tchesnokov, O.S. Volkova, A.N. Vasiliev, V.M. Pudalov, A.V. Sadakov, A.S. Usol'tsev, T. Wolf, E.P. Khlybov, L.F. Kulikova. J. Supercond. Nov. Magn. **26**, *9*, 2867 (2013).
[12] Yu.G. Naidyuk, O.E. Kvitnitskaya, N.V. Gamayunova, D.L. Bashlakov, L.V. Tyutrina, G. Fuchs, R. Hühne, D.A. Chareev, A.N. Vasiliev. Phys. Rev. B **96**, *9*, 094517 (2017).
[13] D.L. Bashlakov, N.V. Gamayunova, L.V. Tyutrina, J. Kačmarčik, P. Szabó, P. Samuely, Y.G. Naidyuk. Low Temp. Phys. **45**, *11*, 1222 (2019).
[14] V.A. Stepanov, M.V. Golubkov, A.V. Sadakov, A.S. Usoltsev, D.A. Chareev. ZhETF, **166**, *5*, 1 (2024). (in Russian).
[15] M. Bristow, A. Gower, J.C.A. Prentice, M.D. Watson, Z. Zajicek, S.J. Blundell, A.A. Haghighirad, A. McCollam, A.I. Coldea. Phys. Rev. B, **108**, *18*, 184507 (2023).
[16] S. Kasahara, Y. Sato, S. Licciardello, M. Čulo, S. Arsenijević, T. Ottenbros, T. Tominaga, J. Böker, I. Eremin, T. Shibauchi, J. Wosnitza, N.E. Hussey, Y. Matsuda. Phys. Rev. Lett. **124**, *10*, 107001 (2020).
[17] I.I. Mazin, D.J. Singh, M.D. Johannes, M.H. Du. Phys. Rev. Lett., **101**, *5*, 057003 (2008).
[18] P.J. Hirschfeld, M.M. Korshunov, I.I. Mazin. Rep. Prog. Phys. **74**, *12*, 124508 (2011).
[19] P. Dai. Rev. Mod. Phys. **87**, *3*, 855 (2015).
[20] W. Ko, S.Y. Song, J. Yan, J.L. Lado, P. Maksymovych. Nano Letters **23**, *17*, 8310 (2023).
[21] A.A. Golubov, M.Yu. Kupriyanov, E. Il'ichev. Rev. Mod. Phys. **76**, *2*, 411 (2004).
[22] A. Barone, G. Paterno. Physics and Applications of the Josephson Effect. John Wiley & Sons, New York (1982). 529 p.
[23] I.B. Sperstad, J. Linder, A. Sudbø. Phys. Rev. B **80**, *14*, 144507 (2009).
[24] Y. Ota, M. Machida, T. Koyama, H. Matsumoto. Phys. Rev. Lett. **102**, *23*, 237003 (2009).
[25] Y. Ota, M. Machida, T. Koyama. Phys. Rev. B **82**, *14*, 140509(R) (2010).
[26] S-Z. Lin. Phys. Rev. B **86**, *1*, 014510 (2012).
[27] F. Romeo, R. Citro. Phys. Rev. B **91**, *3*, 035427 (2015).
[28] A.V. Burmistrova, I.A. Devyatov, A.A. Golubov, K. Yada, Y. Tanaka, M. Tortello, R.S. Gonnelli, V.A. Stepanov, X. Ding, H.-H. Wen, L.H. Greene. Phys. Rev. B **91**, *21*, 214501 (2015).
[29] X. Zhang, Y.S. Oh, Y. Liu, L. Yan, K.H. Kim, R.L. Greene, I. Takeuchi. Phys. Rev. Lett. **102**, *14*, 147002 (2009).
[30] P. Seidel. Supercond. Sci. Tech. **24**, *4*, 043001 (2011).
[31] S. Döring, S. Schmidt, F. Schmidl, V. Tympel, S. Haindl, F. Kurth, K. Iida, I. Mönch, B. Holzapfel, P. Seidel. Supercond. Sci. Tech. **25**, *8*, 084020 (2012).
[32] S. Schmidt, S. Döring, F. Schmidl, V. Grosse, P. Seidel, K. Iida, F. Kurth, S. Haindl, I. Mönch, B. Holzapfel. Appl. Phys. Lett. **97**, *17*, 172504 (2010).
[33] S. Döring, M. Monecke, S. Schmidt, F. Schmidl, V. Tympel, J. Engelmann, F. Kurth, K. Iida, S. Haindl, I. Mönch, B. Holzapfel, P. Seidel. J. Appl. Phys. **115**, *8*, 083901 (2014).
[34] V.V. Fisun, O.P. Balkashin, O.E. Kvitnitskaya, I.A. Korovkin, N.V. Gamayunova, S. Aswartham, S. Wurmehl, Yu.G. Naidyuk. Low Temp. Phys. **40**, *10*, 919 (2014).
[35] X. Zhang, B. Lee, S. Khim, K.H. Kim, R.L. Greene, I. Takeuchi. Phys. Rev. B, **85**, *9*, 094521 (2012).
[36] S. Schmidt, S. Döring, N. Hasan, F. Schmidl, V. Tympel, F. Kurth, K. Iida, H. Ikuta, T. Wolf, P. Seidel. Phys. Status Solidi B **254**, *1*, 1600165 (2017).
[37] M. Tortello, V.A. Stepanov, X. Ding, H.-H. Wen, R.S. Gonnelli, L.H. Greene. J. Supercond. Nov. Magn. **29**, *3*, 679 (2016).
[38] V.A. Stepanov, M.V. Golubkov. JETP, **130**, *2*, 204 (2020).
[39] M.V. Golubkov, V.A. Stepanov, A.V. Sadakov, A.S. Usoltsev, I.V. Morozov. JETP, **136**, *2*, 155 (2023).
[40] D. Chareev, E. Osadchii, T. Kuzmicheva, J.-Y. Lin, S. Kuzmichev, O. Volkova, A. Vasiliev. Cryst. Eng. Comm. **15**, *10*, 1989 (2013).
[41] S. Knöner, D. Zielke, S. Köhler, B. Wolf, Th. Wolf, L. Wang, A. Böhmer, C. Meingast, M. Lang. Phys. Rev. B **91**, *17*, 174510 (2015).
[42] A.E. Böhmer, V. Taufour, W.E. Straszheim, T. Wolf, P.C. Canfield. Phys. Rev. B **94**, *2*, 024526 (2016).
[42] A.A. Sinchenko, P.D. Grigoriev, A.P. Orlov, A.V. Frolov, A. Shakin, D.A. Chareev, O.S. Volkova, A.N. Vasiliev. Phys. Rev. B **95**, *16*, 165120 (2017).
[44] Yu.G. Naidyuk, I.K. Yanson. Point-Contact Spectroscopy. Springer, New York (2005). 297 p.
[45] V.N. Gubankov, K.K. Likharev, N.M. Margolin. FTT **14**, *4*, 953 (1972). (in Russian).
[46] V.N. Gubankov, V.P. Koshelets, G.A. Ovsyannikov. JETP, **44**, *1*, 181 (1976).
[47] L.G. Aslamazov, A.I. Larkin. JETP, **41**, *2*, 381 (1975).
[48] N. Argaman. Superlattices Microstruct. **25**, *5–6*, 861 (1999).
[49] A.N. Vystavkin, V.N. Gubankov, L.S. Kuzmin, K.K. Likharev, V.V. Migulin, V.K. Semenov. Rev. Phys. Appl. **9**, *1*, 79 (1974).
[50] P.G. de Gennes. Rev. Mod. Phys. **36**, *1*, 225 (1964).
[51] M.Yu. Kupriyanov, V.F. Lukichev. Sov. J. Low Temp. Phys. **8**, *10*, 526 (1982).
[52] M.Yu. Kupriyanov, K.K. Likharev, V.F. Lukichev. JETP, **56**, *1*, 235 (1982).
[53] M.Yu. Kupriyanov, A. Brinkman, A.A. Golubov, M. Siegel, H. Rogalla. Physica C **326–327**, 16 (1999).

[54] K.K. Likharev. UFN **127**, *2*, 185 (1979). (in Russian).
[55] V. Ambegaokar, A. Baratoff. Phys. Rev. Lett. **11**, *2*, 104 (1963).
[56] T. Katase, Y. Ishimaru, A. Tsukamoto, H. Hiramatsu, T. Kamiya, K. Tanabe, H. Hosono. Appl. Phys. Lett. **96**, *14*, 142507 (2010).
[57] A.A. Kalenyuk, E.A. Borodianskyi, A.A. Kordyuk, V.M. Krasnov. Phys. Rev. B **103**, *21*, 214507 (2021).
[58] J. Russer. J. Appl. Phys. **43**, *4*, 2008 (1972).
[59] K.K. Likharev, V.K. Semenov. Radiotekhnika i elektronika **16**, *11*, 2167 (1971). (in Russian).
[60] M.V. Golubkov, V.A. Stepanov. Physics of the Solid State, **66**, *4*, 515 (2024).

Translated by M.Verenikina